

## The effect of a thin compliant protective coating on Hertzian contact stresses

M J Matthewson†

Physics and Chemistry of Solids, Cavendish Laboratory, Madingley Road, Cambridge, CB3 0HE, UK

Received 10 July 1981

**Abstract.** When a brittle material is loaded by a blunt indenter a Hertzian cone crack may form in its surface. This crack weakens the material and can lead to material removal. In many practical situations a thin compliant coating may be applied either to deliberately reduce this type of damage or for some other reason (e.g. an anti-corrosion paint layer). This paper models abrasion and impact on the coated system by the contact of a rigid sphere. The results of simple analyses for the stresses within the coating are used to determine how the tensile stresses in the surface of the material, which would lead to Hertzian fracture in the absence of the coating, are modified by the presence of the coating. The two extreme cases of rigid and zero adhesion of the coating to the substrate are directly compared. It is found that the stresses are most sensitive to the coating adhesion, Poisson's ratio and thickness while the modulus of the coating material is only of secondary importance. It is shown that for optimum protection by the coating, it should be rigidly adhering to the substrate, that it should be nearly incompressible (Poisson's ratio  $>0.4$ ) and that the coating thickness should be approximately 20% of the radius of the contact between the coating and the sphere. These criteria allow a protective coating to be designed using theoretical arguments rather than to be developed empirically.

### Nomenclature

$a$	indenter/coating contact radius
$h$	coating thickness
$R$	sphere radius
$G$	coating shear modulus
$\nu$	coating Poisson's ratio
$\nu_s$	substrate Poisson's ratio
$\sigma_2$	principal stress component within the coating normal to its surface
$\tau_0$	radial ( $\tau_{rz}$ ) shear stress at the coating/substrate interface
$\sigma_r, \sigma_\theta$	radial and circumferential stress components in the substrate surface
$\rho$	normalised radial coordinate.

### 1. Introduction

When a blunt indenter is loaded normally on a flat half-space, the radial stress in the surface of the flat has a maximum tensile value at the edge of the contact if there is no

† Present address: University of Cambridge Computer Laboratory, Corn Exchange Street, Cambridge, CB2 3QG, UK.

friction between them (the Hertz analysis) or near this position if there is friction (Johnson *et al* 1973). This stress may lead to the formation of the well known Hertzian cone crack in brittle materials. The crack reduces the strength of the material, degrades the surface condition and may lead to material removal. This is known to be an important mechanism for damage when a body is abraded or impacted by solid particles or liquid masses.

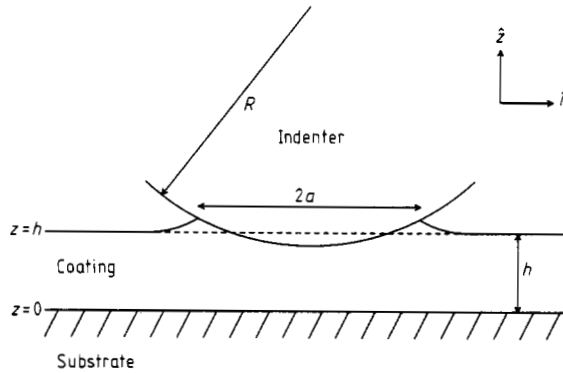


Figure 1. Geometry of the indentation model for abrasion/impact on a coated substrate.

In the practical situation, components of a structure are frequently coated by a thin layer which reduces abrasion or impact damage. The layer may be applied either to deliberately reduce damage or for some other reason, for example a paint layer to prevent corrosion. Protective coatings generally fall into two categories: very hard materials (such as ceramics and hard metal alloys) and very compliant materials (elastomers). This paper is concerned only with compliant coatings whose modulus may be typically a few orders of magnitude lower than that of the substrate which they protect.

The practical situations of abrasion or impact are modelled by the quasi-static loading of a sphere on to the coated system. Figure 1 shows the geometry of the model where a sphere of radius  $R$  is loaded on to a thin layer of thickness  $h$  giving a contact zone of radius  $a$ . Relatively simple analyses for the stresses within the coating have been found for two extreme cases: first when the coating is rigidly attached to the substrate (Matthewson 1981) and secondly when the coating is free to slide over the substrate without friction (Conway *et al* 1970). Both these analyses use the following assumptions:

- (i)  $h < a$  (thin coating approximation);
- (ii)  $R \gg a$  ('blunt' indenter approximation);
- (iii) the indenter and substrate are rigid (compliant coating);
- (iv) the indenter/coating contact is frictionless; and
- (v) the deformation of the coating is governed by the standard linear elasticity equations.

These assumptions allow certain simplifying approximations to be made and the analyses of Matthewson and Conway *et al* produce analytic results. For this reason their analyses are used in this work, rather than more accurate but numerical solutions (e.g. Sneddon 1951, McCormick 1978). Matthewson has shown that his analysis has an accuracy of better than 10% for  $a/h > 2$  and 3% for  $a/h > 5$  and similar accuracy can be expected for the analysis of Conway *et al*.

The solutions for the stresses within the coating are used to calculate how the stresses in the surface of the substrate are modified by the presence of the coating. Matthewson (1979) discusses various mechanisms by which coatings provide protection. The most important is that a compliant coating spreads the contact load, thus reducing the magnitude of stresses in the substrate, but the work presented here demonstrates that the coating adhesion takes a dominant role in this mechanism; the substrate stresses may become predominantly compressive if the coating is adhering. This effect is sensitive to the coating thickness  $h$  and Poisson's ratio  $\nu$ , and is investigated in detail.

**2. Theoretical treatment**

When a sphere is loaded on the coating (figure 1) the substrate will be subjected to two stress distributions transmitted to it via the coating; a normal pressure,  $\sigma_z(r)$ , and a surface traction in the radial direction,  $\tau_0(r)$ . Both stresses produce components of stress within the substrate surface. It is assumed that the effects of  $\sigma_z(r)$  and  $\tau_0(r)$  are independent; they are calculated separately and the resultant stress distributions in the substrate surface are found by linear superposition.

Matthewson finds that for a rigidly bonded coating

$$\left. \begin{aligned} \frac{\tau_0(r) R}{G a} &= \frac{2\nu}{1-2\nu} \frac{r}{a} + \alpha I_1 \left[ \left( \frac{3(1-2\nu)}{2(1-\nu)} \right)^{1/2} \frac{r}{h} \right] & 0 < r < a \\ &= \beta K_1 \left[ \left( \frac{6(1-\nu)}{4+\nu} \right)^{1/2} \frac{r}{h} \right] & r > a \end{aligned} \right\} \quad (1)$$

$$\left. \begin{aligned} \frac{\sigma_z(r) R}{G a} &= \frac{2\nu}{1-2\nu} \left[ \frac{h R}{3 G a} \left( \frac{d\tau_0}{dr} + \frac{\tau_0}{r} \right) - \frac{h}{3a} + \frac{(1-\nu)}{\nu} \left( \frac{r^2 - a^2}{2ha} + \gamma \right) \right] & 0 < r < a \\ &= 0 & r > a \end{aligned} \right\} \quad (2)$$

where the constants  $\alpha$ ,  $\beta$  and  $\gamma$  are obtained by matching the solutions for  $r < a$  and  $r > a$  at the boundary  $r = a$ :

$$\left. \begin{aligned} \alpha &= \frac{(K'a - K)(6\nu - 1)}{2(KI' - IK')(1 - 2\nu)a} \\ \beta &= \frac{4}{(4 + \nu)K'} \left( \frac{(1 - 6\nu)}{2a(1 - 2\nu)} + \alpha I' \right) \\ \gamma &= - \frac{\nu}{1 - \nu} \frac{4 + \nu h}{12 a} \beta (K'a + K) \\ I &= I_1 \left[ \left( \frac{3(1 - 2\nu)}{2(1 - \nu)} \right)^{1/2} \frac{a}{h} \right] & I' &= \frac{dI}{da} \\ K &= K_1 \left[ \left( \frac{6(1 - \nu)}{4 + \nu} \right)^{1/2} \frac{a}{h} \right] & K' &= \frac{dK}{da} \end{aligned} \right\} \quad (3)$$

and where  $I_1(x)$  and  $K_1(x)$  are the first-order modified Bessel functions (see for example Abramowitz and Stegun 1965).

Equations (1)<sub>1</sub> and (2)<sub>1</sub> have an apparent singularity in  $(1 - 2\nu)^{-1}$  but when  $I_1(x)$  is expanded as a power series in  $x$  this singularity disappears. However, numerical evaluation of the equations is not possible at  $\nu = 0.5$ . This problem can be avoided by taking

$\nu = 0.49999$  when the evaluation of the equations is both stable and indistinguishable from an explicit solution for  $\nu = 0.5$  given by Matthewson.

Conway *et al* (1970) find that for a coating which is free to slide over the substrate without friction

$$\frac{\tau_0(r) R}{G a} = 0 \quad \text{for all } r \tag{4}$$

$$\left. \begin{aligned} \frac{\sigma_z(r) R}{G a} &= -\frac{a}{(1-\nu)h} \left(1 - \frac{r^2}{a^2}\right) & 0 < r < a \\ &= 0 & r > a \end{aligned} \right\} \tag{5}$$

Examination of equations (1) to (5) shows that the stresses  $\sigma_z(r)$  and  $\tau_0(r)$  are in both cases proportional to  $G/R$ . This means that all stresses (both in the coating and the substrate) may be normalised to a dimensionless form by the factor  $R/Ga$  and become independent of both  $R$  and  $G$  when in this form.

2.1. Normal load components of stress

When an elastic half-space is subjected to an axisymmetric distribution of load,  $p(\rho)$ , normal to its surface and confined to the region  $0 < \rho < 1$ , then the two components of stress lying in the surface of the half-space may be found by equations given by Johnson *et al* (1973) which are in terms of the Green's function for  $p(\rho)$  (Spence 1968). K L Johnson (private communication) shows that by reversing the order of the double integration produced, these equations simplify and the radial and circumferential stress components at the surface of the substrate are given by

$$\left. \begin{aligned} \sigma_r(\rho) &= \frac{1 - 2\nu_s P(\rho)}{2\pi \rho^2} - p(\rho) & 0 < \rho < 1 \\ &= \frac{1 - 2\nu_s P}{2\pi \rho^2} & \rho > 1 \\ \sigma_\theta(\rho) &= -\frac{1 - 2\nu_s P(\rho)}{2\pi \rho^2} - 2\nu_s p(\rho) & 0 < \rho < 1 \\ &= -\frac{1 - 2\nu_s P}{2\pi \rho^2} & \rho > 1 \end{aligned} \right\} \tag{6}$$

where  $\nu_s$  is the Poisson's ratio of the substrate material and  $P(\rho)$  is the normal load applied within a radius  $\rho$

$$P(\rho) = \int_0^\rho 2\pi\xi p(\xi) d\xi \tag{7}$$

and  $P$  is the total load,  $P(1)$ .

2.2. Surface traction components of stress

The stress components lying in the surface of a half-space produced by an axisymmetric distribution of radial shear traction acting on its surface,  $q(\rho)$  distributed within the

region  $0 < \rho < 1$ , are given by Johnson *et al* (1973):

$$\left. \begin{aligned} \sigma_r(\rho) &= \frac{4}{\pi\rho} \left( \frac{d}{d\rho} - \frac{1 - \nu_s}{\rho} \right) L(\rho) & 0 < \rho < 1 \\ &= \frac{4}{\pi\rho} \left( \frac{d}{d\rho} - \frac{1 - \nu_s}{\rho} \right) L(1) & \rho > 1 \\ \sigma_\theta(\rho) &= \frac{4}{\pi\rho} \left( \nu_s \frac{d}{d\rho} + \frac{1 - \nu_s}{\rho} \right) L(\rho) & 0 < \rho < 1 \\ &= \frac{4}{\pi\rho} \left( \nu_s \frac{d}{d\rho} + \frac{1 - \nu_s}{\rho} \right) L(0) & \rho > 1 \end{aligned} \right\} \quad (8)$$

$$L(\xi) = \int_0^\xi \frac{xM(x)}{(\rho^2 - x^2)^{1/2}} dx \quad (9)$$

where the function  $M(x)$  is defined by Spence (1968):

$$M(x) = x \int_x^1 \frac{q(\rho)}{(\rho^2 - x^2)^{1/2}} d\rho. \quad (10)$$

By considering the substrate of the coated system as an elastic half-space subjected to a loading normal to, and a shear traction along its surface, we may identify  $p(\rho)$  and  $q(\rho)$  with the stresses transmitted to the substrate by the coating, namely,  $\sigma_z(r)$  and  $\tau_0(r)$ .

### 2.3. Rigidly adhering coating

The surface stress components due to the normal loading are found for a rigidly adhering coating by substitution of equations (2) into equations (6) using the relations  $p(\rho) = -\sigma_z(r)$  and  $\rho = r/a$  (the minus sign is introduced here since  $p(\rho)$  is a positive pressure while  $\sigma_z(r)$  is a stress, positive when tensile). The results are not easy to express analytically and will not be stated explicitly. The stresses are calculated by expressing them in terms of the Bessel functions,  $I_1(x)$  and  $K_1(x)$  and then operating on the power series expansion for these functions term by term.

Calculation of the effect of the surface traction is more difficult since the integrations in equations (9) and (10) are not readily treated analytically, but need to be calculated numerically. The function  $q(\rho)$  may be identified with the shear stress  $\tau_0(r)$ . However, equations (8–10) assume that  $q(\rho) = 0$  for  $\rho > 1$ . This condition is not satisfied by  $\tau_0(r)$  which is non-zero everywhere, but converges towards zero for large  $r$ , but since  $\tau_0(r)$  falls rapidly outside the contact region,  $r > a$ , it is assumed that  $\tau_0(r)$  is sensibly zero by  $r = 2a$ . Thus  $q(\rho) = \tau_0(r)$  where in this case  $\rho = r/a'$  where  $a'$  is taken as  $a' = 2a$ .

Although the integral for  $M(x)$  (equation (10)) converges for all  $x$ , the integrand is singular at  $\rho = x$ . The singularity is removed for numerical evaluation by partial integration giving

$$M(x) = -x \int_x^1 \frac{d}{d\rho} \left( \frac{q(\rho)}{\rho} \right) (\rho^2 - x^2)^{1/2} d\rho + xq(1) (1 - x^2)^{1/2}. \quad (11)$$

Values of  $M(x)$  are tabulated and  $M(x)$  and its derivative are found at any point by interpolation. The singularity in the second integration (equation (9)) is removed by the

substitution  $x = \rho \sin \varphi$ , giving

$$L(\xi) = \int_0^{\sin^{-1}(\xi/\rho)} \rho \sin \varphi M(\rho \sin \varphi) d\varphi. \quad (12)$$

Another problem arises when evaluating  $\sigma_r$  and  $\sigma_\theta$  at  $\rho = 0$  because of the factor  $1/\rho$ . However, for small  $x$ ,  $M(x) \approx mx$  ( $m$  is a constant) and  $L(\rho)$  may be found analytically giving

$$\sigma_r(0) = \sigma_\theta(0) = m(1 + \nu_s) \quad (13)$$

where  $m$  can be identified with the gradient of  $M(x)$  at  $x = 0$ .

Both integrations were calculated using the Clenshaw–Curtis method. The stability and accuracy of the results were checked by changing the integration step length, the number of tabulated values of  $M(x)$  and the range of the first integration ( $a' = 2a, 3a, 4a$ ). The error in the results is estimated to be less than 1% which is not significant when compared to the overall accuracy of the theoretical work.

#### 2.4. Non-adhering coating

When there is no adhesion or friction between the coating and the substrate,  $p(\rho)$  is given by  $p(\rho) = -\sigma_z(r)$ ,  $\rho = r/a$ , and  $q(\rho)$  is zero everywhere. By substituting equations (4) into (6), the stress distribution within the substrate surface is given by

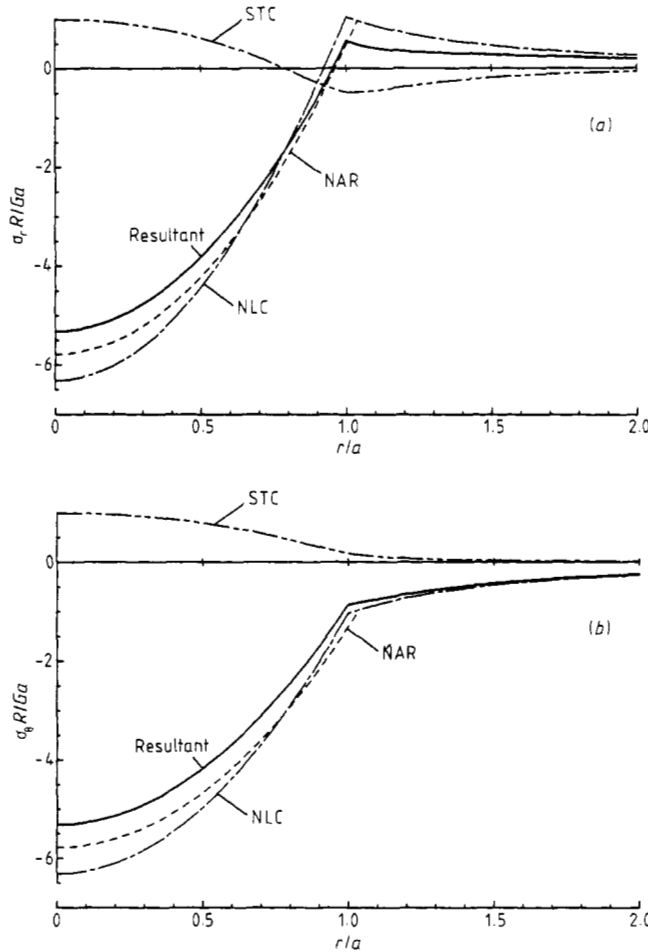
$$\left. \begin{aligned} \frac{\sigma_r(r) R}{G a} &= \frac{a}{4h(1-\nu)} [\rho^2(3+2\nu_s) - 2 - 4\nu_s] & 0 < \rho < 1 \\ &= \frac{a}{4h(1-\nu)} (1-2\nu_s) \frac{1}{\rho^2} & \rho > 1 \\ \frac{\sigma_\theta(r) R}{G a} &= \frac{a}{4h(1-\nu)} \{\rho^2(1+6\nu_s) - 2 - 4\nu_s\} & 0 < \rho < 1 \\ &= \frac{-a}{4h(1-\nu)} (1-2\nu_s) \frac{1}{\rho^2} & \rho > 1. \end{aligned} \right\} \quad (14)$$

### 3. Results

For the case of a rigidly bonded coating, the way in which the resultant of the normal load and surface traction stress components behaves with varying coating parameters is generally complex, but two extremes of behaviour can be identified.

Figure 2 shows the normalised (a) radial and (b) circumferential stress components in the substrate surface calculated for a rigidly adhering coating with  $\nu = 0.3$ ,  $\nu_s = 0.25$  and  $a/h = 5$ . The normal load component of the radial stress (figure 2(a), labelled NLC) is compressive at the centre of the contact ( $r/a = 0$ ) and rises with radius until a maximum is reached at the edge of the contact ( $r/a = 1$ ). Its magnitude decays by an inverse square relation (equation (6)) outside this region. This behaviour is identical in form to that exhibited in the absence of a coating, i.e. Hertzian contact. In contrast, the surface traction component (labelled STC) is tensile at the centre of the contact and falls until a maximum compression is reached near the edge of the contact, after which it decays towards zero at large radii. In this case, which is typical for low Poisson's ratio coatings or low values of  $a/h$ , the maximum tensile stress at the edge of the contact for the normal

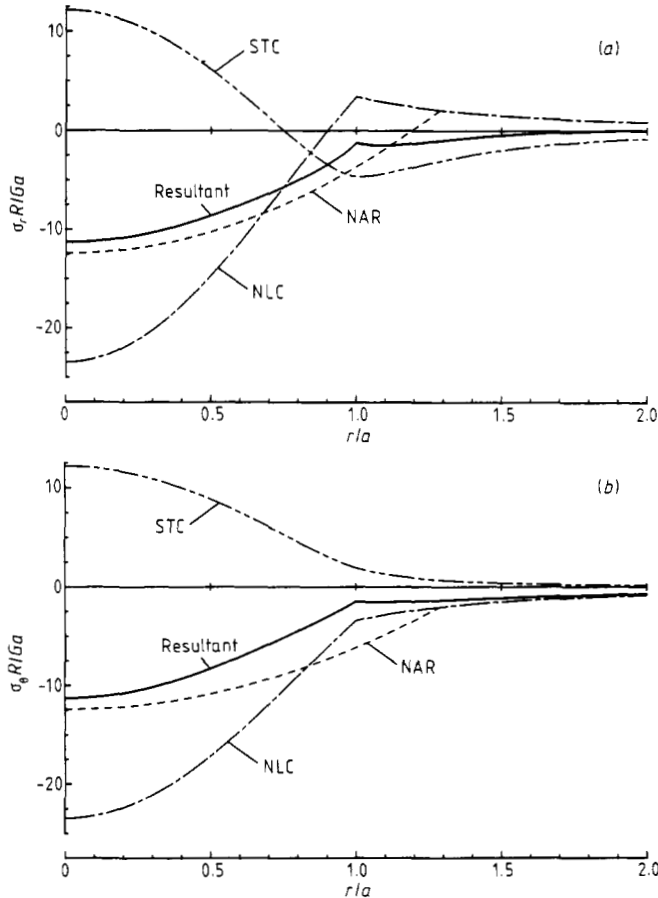
load component dominates over the compression of the surface traction component and the resultant found by summing them (solid curve) behaves in a similar fashion to the normal load component and also has a maximum tensile stress at the contact edge, though of reduced magnitude.



**Figure 2.** Normalised (a) radial and (b) circumferential stress components in the surface of the substrate calculated for  $\nu = 0.3$ ,  $\nu_s = 0.25$  and  $a/h = 5$ . The resultant (solid curve) is the sum of the normal load component (NLC) and the surface traction component (STC). Also shown is the non-adhering coating resultant (NAR) calculated for the same load.

The resultant radial stress for a non-adhering coating (labelled NAR) is also shown. For the purposes of comparison this result is calculated for the same coating subjected to the same total load as the bonded case and  $a/h \neq 5$ . This is so that the effect of the state of adhesion on the substrate stress field can be directly evaluated for identical coatings under identical loading conditions. In this case the coating is more 'compliant' towards the indentation because of fewer constraints on its deformation and a larger contact radius is required to support the same load (about 4% larger than for the bonded coating in this case). Outside the contact region the stress is identical to the normal load

component for the bonded coating (see equation (6)). The maximum tension at the contact edge is approximately twice as large as that for the bonded case. This shows that the adhesion of the coating can significantly reduce the maximum tensile stress in the substrate and will therefore have an important effect on tensile failure of the substrate material.



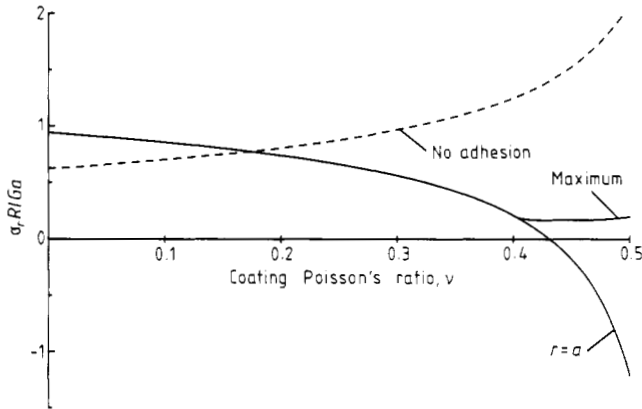
**Figure 3.** Normalised (a) radial and (b) circumferential stress components in the surface of the substrate calculated for  $\nu = 0.5$ ,  $\nu_s = 0.25$  and  $a/h = 5$ .

Figure 2(b) shows the normalised circumferential stress components in the substrate. The surface traction component, while tensile everywhere, has only a small effect compared with the normal load component and the resultants for the bonded and non-adhering cases are both compressive everywhere and do not differ significantly from each other.

The other extreme of behaviour, typical for high Poisson's ratio coatings and large values of  $a/h$ , is shown in figure 3 and is calculated for  $\nu = 0.5$ ,  $\nu_s = 0.25$  and  $a/h = 5$ . Figure 3(a) shows the normalised stress components in the radial direction and it is seen that the forms of the normal load and surface traction components are identical to the previous case. However, the compression of the surface traction component dominates

at the contact edge and the resultant is compressive in this region while for the non-adhering coating (again calculated for the same load) there is a maximum of tension here. In this case the coating adhesion has a profound effect on the probability of tensile failure of the substrate since the radial stress becomes predominantly compressive.

Two other points should be noted in connection with this figure. Firstly, the normal load component always dominates at small radii and the resultant is always compressive at the centre of the contact ( $r = 0$ ). Secondly, it is found that the surface traction component decays more rapidly with radius than the normal load component at large radii. Therefore the resultant radial stress is always tensile at sufficiently large radii; in this case there is a very weak maximum of tension at  $r/a = 2$ .



**Figure 4.** The maximum and contact edge ( $r = a$ ) values of the normalised radial component of stress in the substrate surface as a function of Poisson's ratio,  $\nu$ , calculated for  $\nu_s = 0.25$  and  $a/h = 5$ . Also shown (dashed curve) is the maximum stress for a non-adhering coating under the same loading conditions.

Figure 3(b) shows the circumferential stress components. Again the resultants for both rigidly bonded and non-adhering coatings are compressive everywhere. This result has been found to be general for all cases covered by the theory; the circumferential stress does not play an important role in tensile failure of the substrate and will not be discussed further.

The substrate stresses have been found for a variety of coating parameters and the results are summarised graphically in figures 4 and 5. Figure 4 shows results calculated as a function of  $\nu$  for the bonded coating with  $a/h = 5$  and  $\nu_s = 0.25$ . The solid line (labelled ' $r = a$ ') represents the magnitude of the radial stress in the substrate at the edge of the contact. The curve falls with increasing  $\nu$ ; very rapidly for  $\nu > 0.4$ . The interfacial shear stress,  $\tau_0$ , is extremely sensitive to  $\nu$  for  $\nu > 0.4$  (Matthewson 1981) and therefore the surface traction component of stress plays an increasingly important role as  $\nu$  increases; the increase in the normal load component with  $\nu$  is swamped by this effect. Also shown is the magnitude of the maximum tensile stress in the substrate, which is coincident with the stress at the edge of the contact for  $\nu \leq 0.4$ , but for  $\nu \geq 0.4$  the maximum value lies away from the edge of contact and is roughly independent of  $\nu$ . Also shown in this figure (dashed curve) is the maximum tensile stress in the substrate for a non-adhering coating (which always occurs at the edge of the contact). This curve is calculated for the same applied load as the debonded coating of the same Poisson's

ratio; the ratio  $a/h$  therefore varies along the curve. The curve rises with increasing  $\nu$ , and for  $\nu > 0.2$  the stresses are larger than for the corresponding bonded coating. It may be concluded from this figure that if a protective coating is to be used to minimise the probability of a tensile failure of the substrate then it should be rigidly bonded to the substrate and should have a Poisson's ratio greater than 0.4. Elastomeric materials satisfy the latter condition and for this reason and because of their ability to withstand large strains without failure, they have found widespread use as protective coatings.

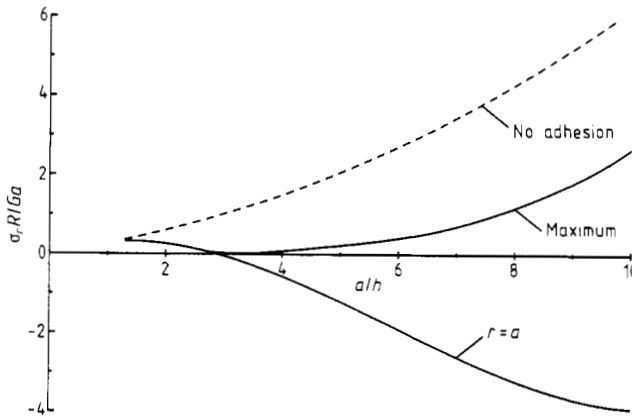


**Figure 5.** The maximum and contact edge ( $r = a$ ) values of the normalised radial component of stress in the substrate surface as a function of  $a/h$  calculated for  $\nu = 0.5$  and  $\nu_s = 0.25$ . Also shown (dashed curve) is the maximum stress for a non-adhering coating under the same loading conditions.

Figure 5 shows the variation of the maximum and contact edge radial stresses as a function of  $a/h$  calculated for a bonded coating with  $\nu = 0.5$  and  $\nu_s = 0.25$ . The analysis for the stresses in the coating is not accurate for  $a/h \leq 2$  but for small  $a/h$  (thick coatings) Hertzian contact on the bulk coating material will be more appropriate. The radial stress at the contact edge initially rises from zero to a maximum as  $a/h$  increases but for  $a/h \geq 2$  it falls and becomes compressive since the surface traction component becomes more dominant, but the maximum value of the radial stress rises for  $a/h \geq 3$  as the surface traction component decays very rapidly with radius for  $r > a$  and a strong maximum is generated outside the contact. The curve for a non-adhering coating (dashed line), calculated for equivalent loading conditions, rises monotonically with  $a/h$  and is everywhere higher than for a bonded coating. Clearly, for the coating to provide optimum protection against tensile failure of the substrate it should be well bonded and the maximum value of  $a/h$  obtained during the loading cycle should be less than about 5 or 6.

Figure 5 shows that for large  $a/h$  the radial stress in the substrate at the edge of the contact for a bonded coating is compressive. In the limit of extremely large  $a/h$  (very thin coatings) one expects the stress field to be Hertzian in form when there will be a tensile stress in this position. Although the present theory would not be valid in this regime since it would require that the substrate strains are no longer negligible compared with those in the coating, there does appear to be a discrepancy. Figure 6 shows details of the resultant radial stress in the substrate near the contact edge calculated for a

bonded coating and  $\nu = 0.5$ ,  $\nu_s = 0.25$  and  $a/h = 6, 8, 10$ . While the stress at  $r = a$  certainly falls with  $a/h$ , it can be seen that the maximum of tension outside the contact is not only increasing in magnitude but is also moving in towards the edge of the contact as  $a/h$  increases. It is therefore plausible to suppose that in the limit of very large  $a/h$  this maximum occurs very near to the edge of the contact and approximates to the Hertzian stress field. Therefore the discrepancy is resolved if the maximum radial stress is considered at large  $a/h$  rather than the stress at  $r = a$ .

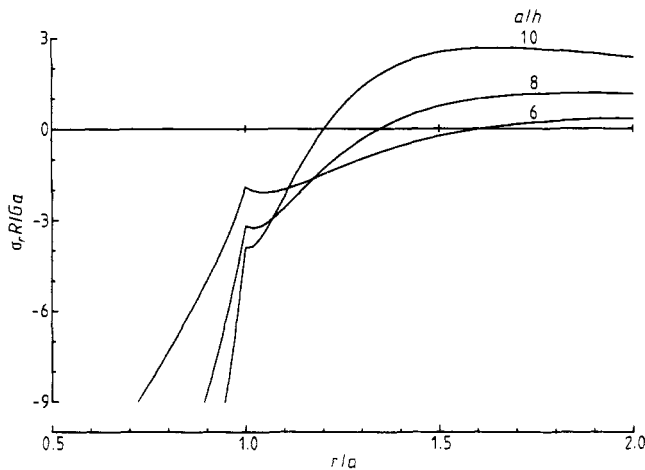


**Figure 6.** Details of the normalised resultant radial stress in the substrate surface for a bonded coating, calculated for  $\nu = 0.5$ ,  $\nu_s = 0.25$  and  $a/h = 6, 8$  and  $10$ .

#### 4. Discussion

It has been seen that the maximum tensile stress occurring in the substrate is a sensitive function of the coating thickness, Poisson's ratio and adhesion. The maximum stress is always lower for a coating that is rigidly adhering (provided  $\nu \geq 0.2$ ). If the coating is adhering the stress is lowest for incompressible coating materials; however, if it is not the stress is largest for these materials. This point is most important since the interfacial shear stress which tends to debond the coating is largest for incompressible coatings and the bond strength needs to be correspondingly greater. The coating/substrate configuration is essentially a cooperative system; the coating protects the substrate by reducing the stress levels in it while the coating is itself protected by its adhesion to the more rigid substrate which restricts the strains that can develop in it. If adhesion is lost then the stresses in the substrate rise, as do the strains in the coating. This change is most dramatic for incompressible coating materials and these materials are more likely to become debonded.

The criterion that the ratio  $a/h$  should not exceed 5 or 6 implies that there is a minimum useful coating thickness. Thinner coatings do not protect the substrate so efficiently and also the interfacial shear stress becomes large and debonding is correspondingly more likely. However, the coating should not be too thick since reinforcement gained by adhesion to the substrate would be lost. There is therefore a range of thicknesses within which the coating must lie.

The elastic modulus of the coating material does not affect the preceding arguments since it only scales the results. However, it does have a secondary importance. In the practical problem of designing a coating, the parameters that can be varied will usually only be the coating thickness and elastic properties since the size of the indenter, the contact load and substrate properties will be determined by the particular situation. Under these circumstances it is possible to obtain the condition on  $a/h$  by manipulating both the coating thickness and elastic modulus; a thick compliant coating can produce the same  $a/h$  ratio as a thinner, more rigid one under the same loading conditions. Unique values for these parameters can only be obtained by applying some other condition. For example, the relative magnitudes of the bond strength and tear strength of the coating might be constrained to equal the relative magnitudes of the maximum interfacial shear stress and the normal stress in the coating in order to simultaneously minimise the probabilities of failure by debonding and tearing. It is worth noting that the ratio of the magnitudes of the interfacial shear stress to the other stresses in the coating are functionally dependent on  $a/h$  and  $\nu$  only, whereas the tear strength and bond strength will in general depend upon the modulus.

The preceding discussion has been confined to brittle substrate materials which fail due to tensile stresses at their surface, but for materials which deform plastically the stresses beneath the surface are relevant. However, the general conclusions concerning surface stresses will apply in this case also because their magnitude reflects the magnitude of the total stress distribution; when the surface stresses are minimised the sub-surface stresses can also be expected to be small.

## 5. Conclusions

An analysis for the stresses in the surface of the substrate of a coated system has elucidated a new mechanism by which a thin compliant coating provides protection. The shear stresses applied to the substrate by a bonded coating set up a stress distribution which opposes the tensile stresses produced by the normal loading. By careful choice of the coating thickness and elastic properties it is possible to minimise the magnitude of tensile stresses to a very low level. To make full use of this mechanism the following conditions should be met:

- (i) the coating should be rigidly bonded to the substrate;
- (ii) the coating Poisson's ratio should exceed 0.4 and the coating should preferably be an elastomer (Poisson's ratio of 0.5) so that large strains can be accommodated by reversible elastic deformation;
- (iii) the maximum contact radius to coating thickness ratio should not exceed 5 or 6.

It is interesting to note that compliant coatings used for protection against solid and liquid impact damage are almost exclusively elastomers which satisfy these criteria. Schmitt (1979) gives a detailed review of this subject. While protective coatings have generally been developed by empirical procedures, this paper suggests criteria which enable effective coatings to be designed on more theoretical grounds.

## Acknowledgments

I thank Dr J E Field (Cavendish Laboratory) for help and advice and Professor K L Johnson (Department of Engineering, University of Cambridge) for useful discussions during the course of this work.

I also thank Churchill College, Cambridge, the Ministry of Defence (Procurement Executive), the Science Research Council and the US Air Office of Scientific Research (grant no. 78-3705) for financial support.

## References

- Abramowitz M and Stegun I E 1965 *Handbook of Mathematical Functions* (New York: Dover) p 374  
Conway H D, Lee H C and Bayer R G 1970 *J. Appl. Mech.* **37** 159–62  
Johnson K L, O'Connor J J and Woodward A C 1973 *Proc. R. Soc. A* **334** 95–117  
Matthewson M J 1979 *Proc. Fifth Int. Conf. on Erosion by Solid and Liquid Impact*, ed. J E Field (Cambridge: University of Cambridge) paper 73  
Matthewson M J 1981 *J. Mech. Phys. Solids*, **29** 89–113  
McCormick J A 1978 *A Numerical Solution for a Generalised Elliptical Contact of Layered Elastic Solids* (MTI report no. 78TR52) (Latham, NY: Mechanical Technology Inc.)  
Schmitt G F 1979 *Liquid and Solid Particle Impact Erosion; Tech. Rep. AFML-TR-79-4122, Wright-Patterson Air Force Base, Ohio*  
Sneddon I N 1951 *Fourier Transforms* (New York: McGraw-Hill) pp 450–510  
Spence D A 1968 *Proc. R. Soc. A* **305** 55–80